Published in final edited form as:

Leukemia. 2017 December ; 31(12): 2652–2660. doi:10.1038/leu.2017.135.

A novel agent SL-401 induces anti-myeloma activity by targeting plasmacytoid dendritic cells, osteoclastogenesis and cancer stem-like cells

A Ray[1], **DS Das**[1], **Y Song**[1], **V Macri**[2], **P Richardson**[1], **CL Brooks**[2], **D Chauhan**[1,3], and **KC Anderson**[1,3]

[1]Department of Medical Oncology, The LeBow Institute for Myeloma Therapeutics and Jerome Lipper Myeloma Center, Dana Farber Cancer Institute, Harvard Medical School, Boston, MA, USA

[2]Stemline Therapeutics, New York, NY, USA

Abstract

Novel therapies for multiple myeloma (MM) can target mechanism(s) in the host-MM bone marrow (BM) microenvironment mediating MM progression and chemoresistance. Our studies showed increased numbers of tumor-promoting, immunosuppressive and drug-resistant plasmacytoid dendritic cells (pDCs) in the MM BM microenvironment. pDC-MM cell interactions upregulate interleukin-3 (IL-3), which stimulates both pDC survival and MM cell growth. Since IL-3 R is highly expressed on pDCs in the MM BM milieu, we here targeted pDCs using a novel IL-3 R-targeted therapeutic SL-401. In both *in vitro* and *in vivo* models of MM in its BM milieu, SL-401 decreases viability of pDCs, blocks pDC-induced MM cell growth, and synergistically enhances anti-MM activity of bortezomib and pomalidomide. Besides promoting pDC survival and MM cell growth, IL-3 also mediates progression of osteolytic bone disease in MM. Osteoclast (OCL) progenitor cells express IL-3 R, and we show that SL-401 abrogates monocyte-derived OCL formation and bone resorption. Finally, we show that SL-401 also decreases the viability of IL-3 R-expressing cancer stem-like cells in MM. Overall, our study provides the preclinical basis for clinical trials of SL-401 to block pDC-induced MM cell growth, inhibit osteoclastogenesis and target MM stem-like cell subpopulations to improve patient outcome in MM.

Correspondence: Dr D Chauhan or Dr KC Anderson, Department of Medical Oncology, The LeBow Institute for Myeloma Therapeutics and Jerome Lipper Myeloma Center, Dana-Farber Cancer Institute, Harvard Medical School, M561, 450 Brookline Ave, Boston, MA 02215, USA. Dharminder_Chauhan@dfci.harvard.edu or Kenneth_Anderson@dfci.harvard.edu.
[3]Joint Senior authors.

CONFLICT OF INTEREST

KCA is on Advisory board of Celgene, Millenium, Gilead and Bristol Myers Squibb, and is a Scientific Founder of Acetylon, Oncopep, and C4 Therapeutics. DC is consultant to Stemline Therapeutic, Inc. The remaining authors declare no conflict of interest.

AUTHOR CONTRIBUTIONS

DC designed the research, analyzed the data and wrote the manuscript; AR performed the experiments and analyzed the data; CLB and VM provided SL-401 and reviewed the manuscript; DSD helped in *in vivo* SCID-hu mouse study and flow cytometry; YS helped in generation of Oct4 cells and flow cytometry; PR provided clinical samples; and KCA analyzed the data and wrote the manuscript.

INTRODUCTION

The bone marrow (BM) microenvironment enhances growth, survival, and drug resistance in multiple myeloma (MM) cells.[1,2] We have shown that interactions of tumor cells with BM accessory cells (BM stromal cells, bone cells, myeloid cells, fibroblasts and immune cells) generates a conducive microenvironment for MM cells to survive, proliferate, evade cytotoxicity of drugs and escape immune responses.[1,3,4] For example, our prior studies demonstrated the functional significance of interactions between MM cells and plasmacytoid dendritic cells (pDCs) in MM pathogenesis.[5,6] Specifically, our studies showed that MM BM pDCs exhibit reduced ability to trigger T-cell proliferation compared to normal pDCs, consistent with the hallmark immune deficiency in MM.[5–8] Our data also showed that increased frequency of pDCs in MM patient BM vs normal BM; and that pDCs are more frequently localized in MM BM than normal BM. Our analysis of clinically-annotated patient samples showed a direct correlation between pDC frequency and disease progression. Importantly, pDCs enhances MM cell growth, survival and drug-resistance.[5] pDCs are relatively resistant to both conventional and novel anti-MM therapies.[5] We showed that pDC-MM interactions enhance secretion of cytokines/chemokines, which mediates both pDC migration and homing to MM BM.[5] Finally, aberrant pDCs function in MM is evidenced not only in their interaction with MM cells, but also with immune effector T and NK cells. For example, MM BM pDCs confer T-cell and natural killer (NK) cell immune suppression in the MM BM milieu.[6] Taken together, our studies therefore provide the basis for development of novel therapies targeting dysfunctional pDCs in MM, both to inhibit MM cell growth and survival and to restore immune function.

Our prior studies demonstrated the role of interleukin 3-receptor (IL-3 R)-mediated signaling during pDC-MM interactions. Specifically, we found that pDC-MM cell interactions significantly increases IL-3 secretion; and importantly, that IL-3 both stimulate pDC survival[9] and MM cell growth.[10] Our and other prior studies showed that pDCs, including MM patient pDCs, highly express IL-3 R.[5,11–13] These findings demonstrate functional significance of IL-3 R-mediated signaling during pDC-MM interactions, and provide the rationale for therapeutically targeting IL-3 R-positive pDCs in MM.

In the current study, we investigated depletion of dysfunctional pDCs as a potential novel therapy in MM. We utilized therapeutic agent SL-401 to target IL-3 R on MM pDCs.[13–15] SL-401 is a recombinant fusion protein composed of human IL-3 fused via a Met-His linker to the catalytic and translocation domains of a truncated diphtheria toxin (DT). The IL-3 domain of SL-401 binds to its cognate receptor (IL-3 R), at which time SL-401 is then internalized, leading to: cleavage of truncated DT from IL-3 within an endosome, translocation of the DT fragment to the cytosol; ADP ribosylation of elongation factor 2; inactivation of protein synthesis; and cell death.[14] Since SL-401 inhibits protein synthesis, it is able to trigger cell death in relatively dormant cells; moreover, it is not a substrate of P-glycoprotein and other drug efflux pumps that are associated with multi-drug resistance. Importantly, clinical activity and a favorable side effect profile of SL-401 has recently been observed in a multicenter Phase I/II trial in patients with advanced hematologic cancers, including blastic plasmacytoid dendritic cell neoplasm (BPDCN), a malignancy of pDC origin.[14–22] Our *in vitro* and *in vivo* studies show that SL-401 inhibits MM cell growth and

survival, inhibits osteoclastogenesis, and targets MM stem-like cells, providing the rationale for its clinical evaluation to improve patient outcome in MM.

MATERIALS AND METHODS

Cell culture

MM cell lines and PBMCs from normal healthy donors were cultured in RPMI-1640 medium supplemented with 10% FBS and antibiotics. Human recombinant IL-3 was purchased from Peprotech Inc (Rocky Hill, NJ, USA). CD3-PE; CD4-FITC or APC-Cy7; CD8-APC, CD123-PE/PE-Cy5/FITC; CD138-FITC/PE/APC; CD133-PE and CD27-Alexa-700 were obtained from BD Biosciences (San Jose, CA, USA). HLA-DR Violet Blue, CD303 (BDCA-2)-FITC, CD14-PE, and CD11c-APC were purchased from Miltenyi Biotec (Auburn, CA, USA); CD304-BV421 was obtained from Biolegend. All immunomagnetic separation kits were purchased from Miltenyi Biotec. Bortezomib, lenalidomide, SAHA, dexamethasone and pomalidomide were purchased from Selleck Chemicals, LLC (Houston, TX, USA).

pDCs and MM cells purification

All studies with MM patient samples were performed in accordance with IRB-approved protocols (Dana-Farber Cancer Institute/Brigham and Women's Hospital, Boston, MA, USA). Helsinki protocol was followed for obtaining informed consent from all patients. pDCs were isolated from both bone marrow (BM) and peripheral blood (PB) mononuclear cells (PBMCs) using CD304 (BDCA-4/Neuropilin-1) microbeads kit (Miltenyi Biotec), and the purity of pDCs (CD3 −, CD14 −, CD19 −, CD20 −, CD56 −, CD11c −, MHC-II/CD123/BDCA-2$^+$) was confirmed, as previously described.[5] The raw data obtained from flow experiments was analyzed using FACS Diva (BD Biosciences) and FlowJO software (ver 7.6.5, Tree Star Inc, Ashland, OR, USA). MM patient cells were purified (>95% purity) by CD138$^+$ selection (CD138 Microbeads kit, Miltenyi Biotec Inc), as previously described.[5,6] CD4$^+$ T cells, CD8$^+$ T cells and monocytes were purified using positive immunomagnetic separation techniques (Ab-Microbeads kits; Miltenyi Biotec).

Isolation of clonogenic MM side population (MM-SP)

MM-SPs were isolated from RPMI-8226 cells by flow cytometry-based Hoechst 33342 staining (5 μg/ml; Ho-33342, Thermo Fisher Scientific, Waltham, MA, USA), as previously described.[23] MM-SPs were identified based on the appearance of scatter shift in Ho-33342 Blue-versus-Red plot, and sorted on FACS Aria-UV flow cytometer (BD Biosciences) with a purity of ~ 99%. For the quantitative analysis of CD123/IL-3Rα$^+$ population, MM-SPs were stained with fluorophore-conjugated anti-CD123/IL-3Rα Abs and analyzed using FACS. In some studies, Vybrant DyeCycle Violet (DCV; Life Technologies Inc, Carlsbad, CA, USA), was used for MM-SPs analyses following the same protocol;[23] circumventing the UV excitation of Hoechst 33342 by utilizing a violet laser for DCV flow analysis.

Cell viability, proliferation, and apoptosis assays

Cell viability and proliferation in MM cell lines, patient MM cells, and normal PBMCs were assessed by MTT or WST assay, as previously described.[24,25] Apoptosis was assessed with

Annexin V-FITC/Propidium iodide apoptosis detection kit (BD Biosciences, San Jose, CA, USA), followed by analysis using FACS Canto II. DNA synthesis was assessed using (3H) thymidine uptake (3H-Tdr) (PerkinElmer, Boston, MA, USA), as previously described.[5] Growth was also assessed by WST assay. For pDCs/MM cells co-culture assays, pDCs and MM cells were cultured at 1:5 pDC/MM ratio.

Osteoclast differentiation and TRAP staining of Monocyte-derived Osteoclasts

Monocytes from PBMC or BMMCs were cultured in the presence of hu-RANKL (40 ng/ml) and hu-M-CSF (25 ng/ml) for 2–3 weeks in RPMI medium. Cells were stained using tartrate-resistant acid phosphatase (TRAP) using TRAP-staining kit (SIGMA, St Louis, MO, USA) for visualization by microscopy. TRAP activity was measured in supernatants at the end of the culture period using a colorimetric substrate included in the TRAP-staining kit (SIGMA). Specifically, supernatants (30 μl) and chromogenic substrate/tartrate-containing buffer (170 μl) were added to each well of a 96-well plate (in triplicate) and incubated at 37 °C for 3 h. TRAP activity was quantified in OCL culture supernatants by absorbance reading at 540 nm. To measure osteoclast resorption, monocytes from PBMCs were cultured in the presence of hu-RANKL (40 ng/ml) and hu-M-CSF (25 ng/ml) for 3 weeks in RPMI medium on OsteoAssay plates, with bone particles at the bottom of the well. Resorbed surface area was analyzed by assessing pit formation. In brief, following multinucleated OCL formation, culture medium was aspirated and cells were washed twice with PBS. Ten percent bleach solution was then added to the wells for 5 min at room temperature followed by washing thrice with distilled water and drying at room temperature for 5 h. The wells were stained with 1% toluidine blue to increase contrast, and pit clusters were observed by microscopy. The images were captured and analyzed using NIH ImageJ software (National Institute of Health (NIH), Bethesda, MD, USA). The bone plus OCL cultures were also subjected to TRAP staining and TRAP activity in supernatants collected from OCL cultures, with or without bone chips, was assessed as described above. CD123/IL-3Rα and CD14 expression on OCL progenitor cells was assessed using FACS.

MM patient BM-derived osteoblast formation and assessment of mineralization

The osteoprogenitor cells (pre-OB) obtained after culturing MM patient BM adherent cells for 3–4 days were stimulated with ascorbic acid (0.05 mg/ ml), β-glycerophosphate (2.16 mg/ml) and 10 nM of dexamethasone for 3 weeks to obtain BM-derived osteoblasts (OBLs). The OBLs were cultured in the presence or absence of indicated concentrations of SL-401, followed by assessment of bone mineralization (calcium deposits) using Alizarin Red staining and Osteogenesis Assay kit (Catalog No. ECM810, Millipore, USA).

Transfection assays

RPMI-8226 and MM-SP cells were transfected with a phOct4-GFP construct using the cell line Nucleofector Kit V (Amaxa Biosystems, Gaithersburg, MD, USA), followed by selection with G418 to derive stable RPMI-8226-Oct4 and MM-SP-Oct4 cell lines. Oct-4/GFP expression was confirmed using FACS.[26]

Animal models

All studies were performed with prior approval from the Institutional Animal Care and Use Committee (DFCI). Subcutaneous MM xenograft model: CB-17 mice were subcutaneously inoculated with MM.1 S cells (2.0×10^6), pDCs (0.4×10^6), or MM.1 S plus pDCs 1:5 (pDC/MM) ratio in 100 μl of serum-free RPMI 1640 medium. When tumors were measurable (300 mm^3), mice (five mice per group) were administered with vehicle alone or SL-401 (16 μg/kg, IV) for 5 consecutive days each week for 2 weeks. Tumor growth was measured as previously described.[24] Kaplan–Meier plots were derived with GraphPad Prism (La Jolla, CA, USA). Human SCID-hu model: This model has been described previously.[27] INA-6 MM cells (2×10^6 cells), alone or together with pDCs (0.4×10^6 cells) at 1:5 (pDC: MM) ratio, were injected directly into the subcutaneously implanted human fetal bone in SCID-hu mice. Upon the first detection of soluble human IL-6 receptor (sIL-6R) in mouse serum, mice were treated with vehicle control or SL-401 (12 μg/kg; IV) for 5 consecutive days for 1 week. Mouse serum samples were analyzed at indicated times for human sIL-6 R (indicative of tumor burden) by ELISA.

Statistics

Student's *t*-test was applied to derive statistical significance. Mice survival was calculated with GraphPad Prism software. Cytotoxic activity of drug combinations was calculated using isobologram analysis and CalcuSyn software program.

RESULTS

Targeting pDCs and pDC-stimulated proliferation of MM cells with novel agent SL-401

Our earlier study showed that IL-3 R-mediated signaling during pDC-MM interactions mediates pDC survival and MM cell growth. pDCs have been reported to express high levels of IL-3 R;[11–13] here we also found that MM patient-derived pDCs ($n = 6$) exhibit high IL-3 R expression (Figure 1a; left and right panels; green color). Moreover, MM cells express IL-3 R as well, albeit at lower levels than pDCs (Figure 1a, left and right panels; blue color). These data identify IL-3 R as a potential therapeutic target primarily on pDCs. In this context, recent research efforts led to the development of a novel therapeutic agent SL-401 (Figure 1b, schematic of SL-401 construction) that specifically targets IL-3 R and IL-3 R-rich pDCs in particular, including the pDC-derived malignancy BPDCN.[13–15]

We first examined the efficacy of SL-401 against pDCs and associated MM cell growth. Freshly purified pDCs and MM cells from patient BM were treated with increasing concentrations of SL-401 for 24 h, and then analyzed for apoptosis. Low picomolar concentrations of SL-401 were sufficient to induce apoptosis in pDCs (>95%; IC_{50}: ~ 13 pM) (Figure 1c). SL-401 also triggers a moderate apoptosis (30 ± 1.3% apoptosis at 1.36 nM) in MM cells, albeit at much higher concentrations (Figure 1c and supplementary Figure 1A, respectively). We next examined the effect of SL-401 on pDCs-induced growth of both MM cell lines and autologous patient MM cells. For pDC-MM co-culture studies, we utilized 1:5 (pDC/MM) ratio, which we established as a physiologically-relevant ratio in our previous study.[5] SL-401 blocked pDCs-triggered proliferation of MM cell lines (Figure 1d and Supplementary Figure S1B), and patient MM cells (Figure 1e) in a concentration-

dependent manner. Importantly, many tumor samples analyzed were obtained from patients with MM refractory to bortezomib, dexamethasone, or lenalidomide. We also examined the effect of SL-401 on cells other than pDCs. As shown in Figure 1f, SL-401 does not significantly decrease the viability of monocytes, $CD4^+$ T cells or $CD8^+$ T cells from MM patients, or PBMCs from normal healthy donors; in contrast, even low concentrations of SL-401 significantly decreased viability of pDCs. These data suggest a favorable therapeutic index for SL-401. Moreover, the normal tissue expression profile of IL-3 R is restricted to certain myeloid progenitors, mature monocytes, eosinophils, basophils, mast cells and pDCs. Importantly, no myelosuppression was noted in previous Phase I/II and phase II trials with SL-401 in patients with BPDCN or relapsed/refractory AML, further supporting the clinical application of SL-401 with a favorable therapeutic index.[14–22]

SL-401 inhibits pDC-induced human MM cell growth *in vivo* and prolongs survival in human MM xenograft models

We first determined the maximum-tolerated dose and toxicity of SL-401. SCID mice were intravenously injected with control vehicle or SL-401 (12 μg/kg, 16 μg/kg, 25 μg/kg or 50 μg/kg) for 5 consecutive days each week for 3 weeks. SL-401 at 16 μg/kg doses were well tolerated, while higher doses resulted in body weight decrease and toxicity (Supplementary Figure S2). We next examined the efficacy of SL-401 (12 μg/kg) in targeting pDCs and pDC-triggered MM cell growth *in vivo* using two distinct murine xenograft model of human MM. The SCID-hu model allows for determining the *in vivo* anti-MM activity of various drugs in the presence of human BM milieu.[5,27] Human fetal bone is subcutaneously implanted in mice, and human MM cells are then injected into the bone, followed by measurement of secreted soluble interleukin-6 receptor (human sIL-6 R) in mouse sera, which serves as tumor growth marker. As in our prior study,[5] we found significantly increased tumor growth in mice injected with pDCs and human MM INA-6 cells than in mice receiving INA-6 cells alone (Figure 2a). Importantly, treatment of mice with SL-401 blocked pDC-induced tumor growth (Figure 2a). Consistent with our *in vitro* data (Figure 1c), SL-401 triggered modest anti-MM activity (Figure 2a). Anti-pDC activity of SL-401 was confirmed using a subcutaneous model of human MM in SCID mice. Similar to our findings in the SCID-hu model, SL-401 inhibited pDC-triggered MM cell growth in subcutaneous MM xenografts as well (Figure 2b). Moreover, survival of SL-401-treated mice was significantly prolonged (Figure 2c). These data demonstrate efficacy of SL-401 in targeting pDCs *in vivo* at doses that are well tolerated.

SL-401 adds to the anti-MM activity of proteasome inhibitor and immunomodulatory drug pomalidomide

On the basis of our findings, we hypothesized that combining SL-401 to target pDCs with agents directly targeting MM cells will allow for both depletion of tumor-promoting pDCs and enhanced killing of tumor cells. Moreover, our prior studies show that combinations will better target pDCs, which are resistant to anti-MM therapies, as well as confer resistance and promote MM cell growth.[5] For example, our earlier study showed that pDCs are relatively resistant to bortezomib and block bortezomib-induced MM cell cytotoxicity;[5] conversely, combination of SL-401 may restore bortezomib-sensitivity in MM cells. Indeed, we here found that low concentrations of SL-401 combined with bortezomib triggers synergistic

anti-MM cytotoxicity (Supplementary Figure S3). In an analogous manner, we examined the combination of SL-401 with second-generation immunomodulatory agent (IMiD) pomalidomide,[28] which is FDA approved to treat relapsed refractory MM. We reported earlier that pDCs are resistant to first generation IMiD lenalidomide;[5] however, the effect of pomalidomide on pDCs is unknown. Cytotoxicity analysis showed that MM patient pDCs are relatively resistant to pomalidomide treatment as well (Figure 3a). These findings were confirmed using plasmacytoid dendritic[29] cell line CAL-1 (Figure 3b). Similar to MM-pDCs, Cal-1 induces MM cell growth in co-culture model (Supplementary Figure S4). Isobologram analysis showed that the combination of low concentrations of SL-401 with pomalidomide triggers synergistic anti-MM cytotoxicity (Figures 3c and d, and Supplementary Figures S5A–B). We also evaluated the efficacy of combined SL-401 and pomalidomide *in vivo* using our SCID-human (SCID-hu) mouse model. Mice were treated with vehicle control, SL-401 (12 μg/kg; IV), pomalidomide (2.5 mg/kg; orally) or SL-401 plus pomalidomide for 2 weeks (SL-401: 5 consecutive days for first 1 week; pomalidomide: 4 consecutive days weekly for 2 weeks). Significant inhibition of tumor growth was observed in mice treated with SL-401 plus pomalidomide versus mice receiving either agent alone (Figure 3e). These *in vivo* data confirm our *in vitro* findings showing efficacy of SL-401, alone or in combination with pomalidomide.

SL-401 inhibits osteoclast formation and bone resorption, as well as stabilizes osteoblast formation

As noted above, pDC-MM interactions enhance IL-3 secretion, which in turn promotes both pDC survival and MM cell growth. IL-3 also contributes to progression of osteolytic bone disease in MM by stimulating osteoclast (OCL) formation[3,4,30–32] and inhibiting osteoblast differentiation.[31] Previous studies showed that OCL progenitor cells express IL-3 R;[30–32] consistent with these findings, we here demonstrate IL-3 R expression on OCL progenitor cells (Figure 4a). We next examined whether SL-401 affects the OCL formation. Specifically, monocytes from MM patient PBMCs were cultured with hu-M-CSF and hu-RANKL for 2 weeks to promote OCL differentiation, in the presence or absence of SL-401. OCLs were analyzed for tartrate-resistant acid phosphatase (TRAP) staining. As seen in Figure 4b, SL-401 decreased $TRAP^+$ cells versus control cultures. Consistent with these data, supernatants from SL-401-treated OCLs cultures showed significantly decreased TRAP activity (Figure 4c). Examination with OsteoAssay plates (dentine discs) similarly showed inhibitory activity of SL-401 against OCL-mediated bone resorption (Figures 4d and e). These data suggest that SL-401 inhibits monocyte-derived OCL formation and bone resorption.

We also examined whether SL-401 affects osteoblast differentiation. For these studies, we utilized osteoprogenitor cells (pre-OB) obtained by culturing MM patient BM adherent cells for 3–4 days. These cells were stimulated with ascorbic acid/β-glycerophosphate/dexamethasone for 3–4 weeks in the presence and absence of SL-401, followed by analysis for bone mineralization using Alizarin Red staining. SL-401 promotes BM-derived osteoblast formation (Figure 4f). Taken together, these findings support the clinical relevance of SL-401, since it may both block pDC-induced MM cell growth and abrogate osteolytic bone disease in MM.

SL-401 targets tumor-initiating stem-like cells in MM

Our and other prior studies identified clonogenic MM side population cells (MM-SPs), which exhibit stem-cell like features and contribute to relapse of MM.[23,33] Although we showed that lenalidomide decreases MM-SP fraction,[23] therapies targeting MM-SP cells are lacking. We here examined the effect of SL-401 on MM-SP cells since: (1) A recent study showed that IL-3 R serves as a leukemia stem cell marker that predicts minimum residual disease and relapse in acute myeloid leukemia; and importantly, SL-401 targets these cells;[34,35] (2) MM patient BM has elevated IL-3 levels;[31] and (3) pDC-MM interactions significantly increase IL-3 levels, confirming an active IL-3/IL-3 R signaling axis in the MM BM milieu. MM-SPs were isolated from RPMI-8226 and Dox-40 MM cell line, as previously described,[23] and analyzed for IL-3 R expression. As shown in Figure 5, both (A) RPMI-8226- and (C) Dox-40-derived MM-SPs exhibit higher IL-3 R levels versus parental RPMI-8226 cells. Cytotoxicity assays showed a significantly lower IC_{50} of SL-401 against MM-SPs versus MM cells. (Figure 5b: (IC_{50}: 350 pM/ 0.35 nM) versus RPMI-8226 cells (IC_{50}: 1367 pM/1.37 nM); Figure 5d: (IC_{50}: ~ 0.45 nM) versus Dox-40 cells (IC_{50}: ~ 3.6 nM)); pDCs served as a positive control with lowest IC_{50} (Figures 5b and d; IC_{50}: 30 pM/ 0.03 nM).[35] MM-SPs were also analyzed for additional MM cell lines (KMS-11, OPM2 and NCI-H929). MM-SPs derived from KMS-11, OPM2 and NCI-H929 MM cells also exhibited higher IL-3 R levels versus respective parental cells, and cytotoxicity assays showed a significant dose-dependent decrease of viable MM-SPs after SL-401 treatment (Supplementary Figures S6A–C). These data demonstrate the ability of SL-401 to target MM-SPs.

To further examine the anti-cancer stem-like cell activity of SL-401, we stably transfected stem-cell transcription factor Oct-4 into RPMI-8226 MM cells and MM-SPs. Oct-4 mediates drug-resistance and stem-like cell characteristics.[26] Specifically, RPMI-8226 and MM-SP cells were transfected with a phOct4-GFP construct[26] and selected with G418 to derive stable RPMI-8226-Oct4 and MM-SP-Oct4 cell lines (see Supplemntary Figure S7). Using these cell lines, we examined the following: (1) whether surface markers associated with stem cells (CD123/IL-3 Rα, CD133 and CD27) are increased in Oct-4-transfected cells and (2) whether Oct-4-transfected cells become more sensitive to SL-401 treatment. As expected, Oct-4 transfection led to increased expression of stem cell markers IL-3R, CD133 or CD27 versus parental RPMI-8226 cells or MM-SPs (Figures 6a–c). Of note, cytotoxicity analysis showed that RPMI-8226-Oct4, but not parental RPMI-8226 cells, were resistant to proteasome inhibitor bortezomib (Figure 6d). Finally, Oct-4 transfection led to increased sensitivity to SL-401 treatment (IC_{50}: pDCs: 30 pM; MM-SP-Oct4 cells: 50 nM; RPMI-8226-Oct4 cells: 75 pM; MM-SP cells: 350 pM; RPMI-8226 cells: 1367 pM). Taken together, our data indicate that SL-401 targets the cancer stem-like cells in MM.

DISCUSSION

Therapies targeting the MM cell in its BM microenvironment have transformed MM treatment and prolonged patient survival.[1,2] However, relapse of MM occurs in many patients, and delineation of the mechanisms in the BM milieu mediating tumor cell growth, survival and drug resistance, as well as immune suppression can identify and validate

potential novel therapeutic targets. Our prior studies identified the role of increased numbers of plasmacytoid dendritic cells (pDCs) in the MM BM as novel mechanisms both promoting tumor and suppressing host immunity.[5] The present study builds upon our prior results, and preclinically validates a novel therapeutic SL-401 to target and transiently deplete dysfunctional pDCs in MM. SL-401 has shown promising results in a multicenter Phase I/II trial in patients with blastic plasmacytoid dendritic cell neoplasm (BPDCN), a malignancy derived from pDCs, with a favorable toxicity profile and we here examined its preclinical effects using our *in vitro* and *in vivo* models of MM in the BM microenvironment.

Using *in vitro* pDC-MM co-culture model and human MM xenografts, we show that SL-401 decreases viability of drug-resistant pDCs, which express IL-3 R and blocks pDC-induced MM cell growth. We also examined whether SL-401 targets other IL-3 R-expressing cells besides pDCs. In this context, previous studies demonstrated that IL-3 R is restricted to certain myeloid progenitors, mature monocytes, eosinophils, basophils, mast cells and pDCs.[36] In our study, we found no significant effect of SL-401 on the viability of monocytes, B cells or total PBMCs. Although SL-401 would target normal pDCs, adverse immune effects or immunosuppression has not been observed in the clinical studies[14,15] to date, likely due to the restoration of normal pDCs post-SL-401 treatment. Importantly, SL-401 has already demonstrated tolerability, clinical activity and a favorable safety profile without myelosuppression in clinical trials of patients with relapsed AML and BPDCN.[14–22] Together, these findings suggest a favorable therapeutic index for SL-401.

We utilized two distinct human MM xenograft models to show that administration of clinically-achievable doses of SL-401 target pDCs *in vivo* and reduce pDC-mediated tumor growth. Moreover, no significant toxicity was observed in SL-401-treated mice. Since pDCs are resistant to anti-MM agents bortezomib and pomalidomide and protect MM cells against their cytotoxic effects, we hypothesized that SL-401-mediated depletion of dysfunctional pDCs may restore tumor sensitivity to bortezomib- or pomalidomide. Indeed, our combination studies showed that SL-401 synergistically enhanced the anti-MM activity of both bortezomib and pomalidomide. A similar synergy between SL-401 and anticancer agent cytarabine has been reported in leukemia xenograft models.[37] Our findings therefore support clinical trials of SL-401 with bortezomib and/or pomalidomide, in relapsed MM.

We showed that pDC-MM interactions enhance IL-3 levels; and importantly, that IL-3/IL-3 R signaling plays a role in osteolytic bone disease. Here we found that SL-401 inhibits osteoclast formation, bone resorption, and promotes osteoblast formation. Our data therefore provide the first evidence for the anti-osteolytic activity of SL-401, which may serve as novel therapeutic strategy to prevent MM-associated bone disease.

We also identified a significant number of clonogenic side population cells in MM (MM-SPs) with characteristic stem cell-like features, which also express IL-3 R. A previous study similarly showed overexpression of IL-3 R on leukemic cancer stem cells (CSCs).[38,39] Importantly, our studies demonstrated that SL-401 decreased the viability of IL-3 R expressing MM-SPs. Due to the paucity of MM-SPs in BM mononuclear cells from patients or MM cell lines, we derived stable MM cell lines expressing Oct-4 transcription factor, which promotes stemness and chemoresistance. A significant increase in the expression of

stem cell markers (IL-3 R, CD133 and CD27) was noted in Oct-4-transfected- versus non-transfected MM cells, which correlated with increased sensitivity of these cells to SL-401. A recent study also demonstrated anti-CSC activity of SL-401 in advanced CML.[40] Together, our data suggests that SL-401 may target tumor-initiating stem-like cells and thereby abrogate development of drug-resistance in MM.

In summary, we here show that SL-401: (1) decreases the viability of immunologically-defective and tumor-promoting pDCs; (2) blocks pDC-induced MM cell growth; (3) synergistically enhances the anti-MM activity of anti-MM agents bortezomib and pomalidomide; (4) inhibits OCL formation and bone resorption; (5) promotes osteoblast formation and (6) decreases viability of IL-3 R-expressing cancer stem-like cells in MM. These preclinical data provide the rationale for clinical trials of SL-401, alone and in combination with pomalidomide or bortezomib, to overcome pDC-mediated both drug-resistance and MM progression, prevent osteolytic bone disease, deplete tumor-initiating stem cell-like subpopulations and improve patient outcome in MM. A clinical trial of SL-401 in MM is currently ongoing (NCT02661022).

Supplementary Material

Refer to Web version on PubMed Central for supplementary material.

Acknowledgments

The grant support for this investigation was provided by National Institutes of Health Specialized Programs of Research Excellence (SPORE) grant P50100707, R01CA207237, and RO1 CA050947. KCA is an American Cancer Society Clinical Research Professor.

References

1. Anderson KC. The 39th David A. Karnofsky Lecture: bench-to-bedside translation of targeted therapies in multiple myeloma. J Clin Oncol. 2012; 30:445–452. [PubMed: 22215754]
2. Anderson KC. Multiple myeloma. Hematol Oncol Clin North Am. 2014; 28:xi–xii. [PubMed: 25212892]
3. Tai YT, Acharya C, An G, Moschetta M, Zhong MY, Feng X, et al. APRIL and BCMA promote human multiple myeloma growth and immunosuppression in the bone marrow microenvironment. Blood. 2016; 127:3225–3236. [PubMed: 27127303]
4. An G, Acharya C, Feng X, Wen K, Zhong M, Zhang L, et al. Osteoclasts promote immune suppressive microenvironment in multiple myeloma: therapeutic implication. Blood. 2016; 128:1590–1603. [PubMed: 27418644]
5. Chauhan D, Singh AV, Brahmandam M, Carrasco R, Bandi M, Hideshima T, et al. Functional interaction of plasmacytoid dendritic cells with multiple myeloma cells: a therapeutic target. Cancer Cell. 2009; 16:309–323. [PubMed: 19800576]
6. Ray A, Das DS, Song Y, Richardson P, Munshi NC, Chauhan D, et al. Targeting PD1-PDL1 immune checkpoint in plasmacytoid dendritic cell interactions with T cells, natural killer cells and multiple myeloma cells. Leukemia. 2015; 29:1441–1444. [PubMed: 25634684]
7. Brown RD, Pope B, Murray A, Esdale W, Sze DM, Gibson J, et al. Dendritic cells from patients with myeloma are numerically normal but functionally defective as they fail to up-regulate CD80 (B7-1) expression after huCD40LT stimulation because of inhibition by transforming growth factor-beta1 and interleukin-10. Blood. 2001; 98:2992–2998. [PubMed: 11698282]

8. Ratta M, Fagnoni F, Curti A, Vescovini R, Sansoni P, Oliviero B, et al. Dendritic cells are functionally defective in multiple myeloma: the role of interleukin-6. Blood. 2002; 100:230–237. [PubMed: 12070032]
9. Grouard G, Rissoan MC, Filgueira L, Durand I, Banchereau J, Liu YJ. The enigmatic plasmacytoid T cells develop into dendritic cells with interleukin (IL)-3 and CD40-ligand. J Exp Med. 1997; 185:1101–1111. [PubMed: 9091583]
10. Lee JW, Chung HY, Ehrlich LA, Jelinek DF, Callander NS, Roodman GD, et al. IL-3 expression by myeloma cells increases both osteoclast formation and growth of myeloma cells. Blood. 2004; 103:2308–2315. [PubMed: 14615378]
11. Liu Y, Xia D, Li F, Zheng C, Xiang J. Intratumoral administration of immature dendritic cells following the adenovirus vector encoding CD40 ligand elicits significant regression of established myeloma. Cancer Gene Ther. 2005; 12:122–132. [PubMed: 15565183]
12. Reizis B, Bunin A, Ghosh HS, Lewis KL, Sisirak V. Plasmacytoid dendritic cells: recent progress and open questions. Annu Rev Immunol. 2011; 29:163–183. [PubMed: 21219184]
13. Angelot-Delettre F, Roggy A, Frankel AE, Lamarthee B, Seilles E, Biichle S, et al. In vivo and in vitro sensitivity of blastic plasmacytoid dendritic cell neoplasm to SL-401, an interleukin-3 receptor targeted biologic agent. Haematologica. 2015; 100:223–230. [PubMed: 25381130]
14. Frankel AE, Woo JH, Ahn C, Pemmaraju N, Medeiros BC, Carraway HE, et al. Activity of SL-401, a targeted therapy directed to interleukin-3 receptor, in blastic plasmacytoid dendritic cell neoplasm patients. Blood. 2014; 124:385–392. [PubMed: 24859366]
15. Frankel AE, Konopleva M, Hogge D, Rizzieri D, Brooks C, Cirrito T, et al. Activity and tolerability of SL-401, a targeted therapy directed to the interleukin-3 receptor on cancer stem cells and tumor bulk, as a single agent in patients with advanced hematologic malignancies. J Clin Oncol. 2013; 31(15 Suppl):7029.
16. Pemmaraju N, Lane AA, Sweet KL, Stein AS, Vasu S, Blum WG, et al. Results from phase 2 registration trial of SL-401 in patients with blastic plasmacytoid dendritic cell neoplasm (BPDCN): Lead-in completed, expansion stage ongoing.2016 ASCO Annual Meeting. J Clin Oncol. 2016; 34(suppl) abstr 7006.
17. Lane AA, Sweet KL, Wang ES, Donnellan WB, Walter RB, Stein AS, et al. Results from ongoing phase 2 trial of SL-401 as consolidation therapy in patients with acute myeloid leukemia (AML) in remission with high relapse risk including minimal residual disease (MRD). ASH, 2016. Blood. 2016; 128:215.
18. Mani R, Goswami S, Gopalakrishnan B, Ramaswamy R, Wasmuth R, Tran M, et al. SL-401 mediates potent cytotoxicity against CD123+ AML and MDS with excess blasts and demonstrates therapeutic benefit in PDX model. Blood. 2016; 128:580.
19. Gionco J, Chen J, Lindsay R, Macri V, Brooks CL. SL-401, a targeted therapy directed to the interleukin-3 receptor (CD123), and SL-801, a reversible inhibitor of exportin-1 (XPO1), display synergistic anti-tumor activity against hematologic malignancies in vitro. Blood. 2016; 128:4724.
20. Pemmaraju N, Lane AA, Sweet KL, Stein AS, Vasu S, Blum W, et al. Results from Phase 2 trial ongoing expansion stage of SL-401 in patients with blastic plasmacytoid dendritic cell neoplasm (BPDCN). 2016. Blood. 2016; 128:342.
21. Htut M, Gasparetto C, Zonder J, Martin TG III, Scott EC, Chen J, et al. Results from ongoing phase 1/2 trial of SL-401 in combination with pomalidomide and dexamethasone in relapsed or refractory multiple myeloma. Blood. 2016; 128:5696.
22. Patnaik MM, Gupta V, Gotlib JR, Carraway HE, Wadleigh M, Schiller G, et al. Results from ongoing phase 2 trial of SL-401 in patients with advanced, high-risk myeloproliferative neoplasms including chronic myelomonocytic leukemia. Blood. 2016; 128:4245.
23. Jakubikova J, Adamia S, Kost-Alimova M, Klippel S, Cervi D, Daley JF, et al. Lenalidomide targets clonogenic side population in multiple myeloma: pathophysiologic and clinical implications. Blood. 2011; 117:4409–4419. [PubMed: 21321360]
24. Chauhan D, Tian Z, Nicholson B, Kumar KG, Zhou B, Carrasco R, et al. A small molecule inhibitor of ubiquitin-specific protease-7 induces apoptosis in multiple myeloma cells and overcomes bortezomib resistance. Cancer Cell. 2012; 22:345–358. [PubMed: 22975377]

25. Ray A, Tian Z, Das DS, Coffman RL, Richardson P, Chauhan D, et al. A novel TLR-9 agonist C792 inhibits plasmacytoid dendritic cell-induced myeloma cell growth and enhance cytotoxicity of bortezomib. Leukemia. 2014; 28:1716–1724. [PubMed: 24476765]
26. Gerrard L, Zhao D, Clark AJ, Cui W. Stably transfected human embryonic stem cell clones express OCT4-specific green fluorescent protein and maintain self-renewal and pluripotency. Stem Cells. 2005; 23:124–133. [PubMed: 15625129]
27. Tassone P, Neri P, Carrasco DR, Burger R, Goldmacher VS, Fram R, et al. A clinically relevant SCID-hu in vivo model of human multiple myeloma. Blood. 2005; 106:713–716. [PubMed: 15817674]
28. Richardson PG, Siegel D, Baz R, Kelley SL, Munshi NC, Laubach J, et al. Phase 1 study of pomalidomide MTD, safety, and efficacy in patients with refractory multiple myeloma who have received lenalidomide and bortezomib. Blood. 2013; 121:1961–1967. [PubMed: 23243282]
29. Maeda T, Murata K, Fukushima T, Sugahara K, Tsuruda K, Anami M, et al. A novel plasmacytoid dendritic cell line, CAL-1, established from a patient with blastic natural killer cell lymphoma. Int J Hematol. 2005; 81:148–154. [PubMed: 15765784]
30. Silbermann R, Bolzoni M, Storti P, Guasco D, Bonomini S, Zhou D, et al. Bone marrow monocyte-/macrophage-derived activin A mediates the osteoclastogenic effect of IL-3 in multiple myeloma. Leukemia. 2014; 28:951–954. [PubMed: 24369304]
31. Ehrlich LA, Chung HY, Ghobrial I, Choi SJ, Morandi F, Colla S, et al. IL-3 is a potential inhibitor of osteoblast differentiation in multiple myeloma. Blood. 2005; 106:1407–1414. [PubMed: 15878977]
32. Tai YT, Chang BY, Kong SY, Fulciniti M, Yang G, Calle Y, et al. Bruton tyrosine kinase inhibition is a novel therapeutic strategy targeting tumor in the bone marrow microenvironment in multiple myeloma. Blood. 2012; 120:1877–1887. [PubMed: 22689860]
33. Matsui W, Huff CA, Wang Q, Malehorn MT, Barber J, Tanhehco Y, et al. Characterization of clonogenic multiple myeloma cells. Blood. 2004; 103:2332–2336. [PubMed: 14630803]
34. Han L, Rowinsky E, Brooks C, Zal T, Zal MA, Burks JK, et al. Anti-leukemia efficacy and mechanisms of action of SL-101, a novel anti-CD123 antibody-conjugate in acute myeloid leukemia. Blood. 2014; 124:981.
35. Lasho T, Finke C, Kimlinger TK, Zblewski D, Chen D, Patnaik MM, et al. Expression of CD123 (IL-3 R-alpha), a therapeutic target of SL-401, on myeloproliferative neoplasms. Blood. 2014; 124:5577.
36. Brooks CR, van Dalen CJ, Hermans IF, Douwes J. Identifying leukocyte populations in fresh and cryopreserved sputum using flow cytometry. Cytometry B Clin Cytom. 2013; 84:104–113. [PubMed: 23341171]
37. Hogge DE, Feuring-Buske M, Gerhard B, Frankel AE. The efficacy of diphtheria-growth factor fusion proteins is enhanced by co-administration of cytosine arabinoside in an immunodeficient mouse model of human acute myeloid leukemia. Leuk Res. 2004; 28:1221–1226. [PubMed: 15380349]
38. Konopleva M, Hogge DE, Rizzieri DA, Cirrito TP, Kornblau SM, Borthakur G, et al. SL-401, a targeted therapy directed to the interleukin-3 receptor present on leukemia blasts and cancer stem cells, is active as a single agent in patients with advanced AML. Blood. 2012; 120:3625. [PubMed: 22898606]
39. Pinnamaneni P, Jorgensen JL, Kantarjian HM, Jabbour E, Pierce SR, Brandt M, et al. Persistence of minimal residual disease assessed by multi-parameter flow cytometry (MFC) at 30 and 90 days after achieving complete remission predicts outcome in patients with acute myeloid leukemia. Blood. 2014; 124:1015.
40. Frolova O, Benito J, Brooks C, Wang RY, Korchin B, Rowinsky EK, et al. SL-401 and SL-501, targeted therapeutics directed at the interleukin-3 receptor, inhibit the growth of leukaemic cells and stem cells in advanced phase chronic myeloid leukemia. Br J Haematol. 2014; 166:862–874. [PubMed: 24942980]

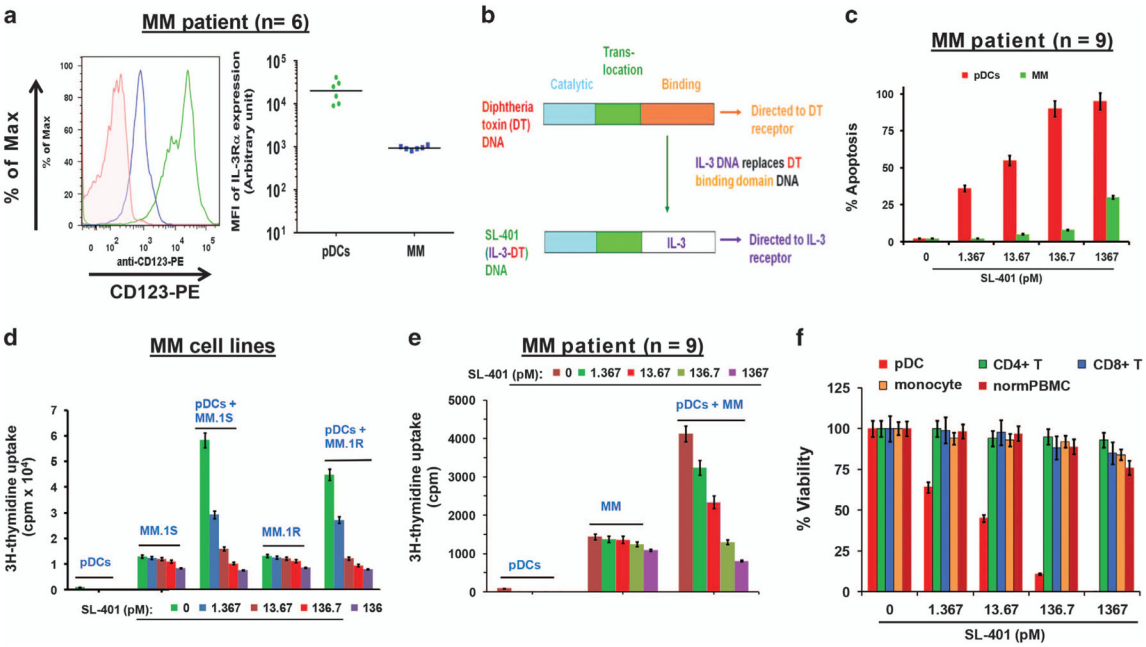

Figure 1.

Effect of SL-401 on pDCs, MM cells and pDC-induced MM cell growth. (**a**) pDC (green) and MM (blue) cells were stained with anti-IL-3 Rα-PE antibody or matched isotype control and analyzed by flow cytometry. (Number of patient samples =6). Left panel: A representative histogram shows IL-3Rα/CD123 expression on pDCs (green) and MM cells (blue). Right panel: Frequency of IL-3 Rα/CD123 expression on patient pDCs and tumor cells. The data is presented as mean fluorescence intensity (MFI) of IL-3Rα/CD123 expression on pDCs (green closed circles) and MM cells (blue closed circles) isolated from patient BM samples (n =6). MFI is shown for each cell type (P<0.0101 for pDCs versus MM cells) (**b**) Schematic of SL-401 construction: SL-401 is a targeted therapy directed to IL-3R consisting of IL-3 fused to a truncated DT payload. The IL-3 domain of SL-401, which replaces the binding domain of DT, targets SL-401 to cells that express the IL-3R. (**c**) Purified pDCs and MM cells from patients (n =9) BM were treated with indicated concentrations of SL-401 for 48 h, and analyzed for apoptosis (IC_{50} for pDCs: 0.83 ng/ml =13.67 picomolar) (mean ±s.d., P<0.005; n =4). (**d**) MM.1 S cells (5×10^4 cells per 200 μl), MM.1 R (5×10^4 cells per 200 μl), and pDCs (1×10^4 cells per 200 μl) were cultured either alone or together (1:5 pDC:MM ratio) for 72 h in the presence or absence of indicated concentrations of SL-401, and DNA synthesis was measured by ^{3}H-TdR uptake (mean ±s.d., n =3). (**e**) Patient (n = 9) MM cells were cultured with or without autologous pDCs for 72 h in the presence or absence of indicated concentrations of SL-401, and DNA synthesis was measured by ^{3}H-TdR uptake (mean ±s.d. of triplicate cultures; P<0.004 for all samples). (**f**) Purified indicated cell types from MM patient (n =5) and total PBMCs from normal donors (n =4) were treated with DMSO vehicle or SL-401 for 72 h and analyzed for viability (mean ±s.d. of quadruplicate cultures). Anti-pDC activity of SL-401 served as a positive control.

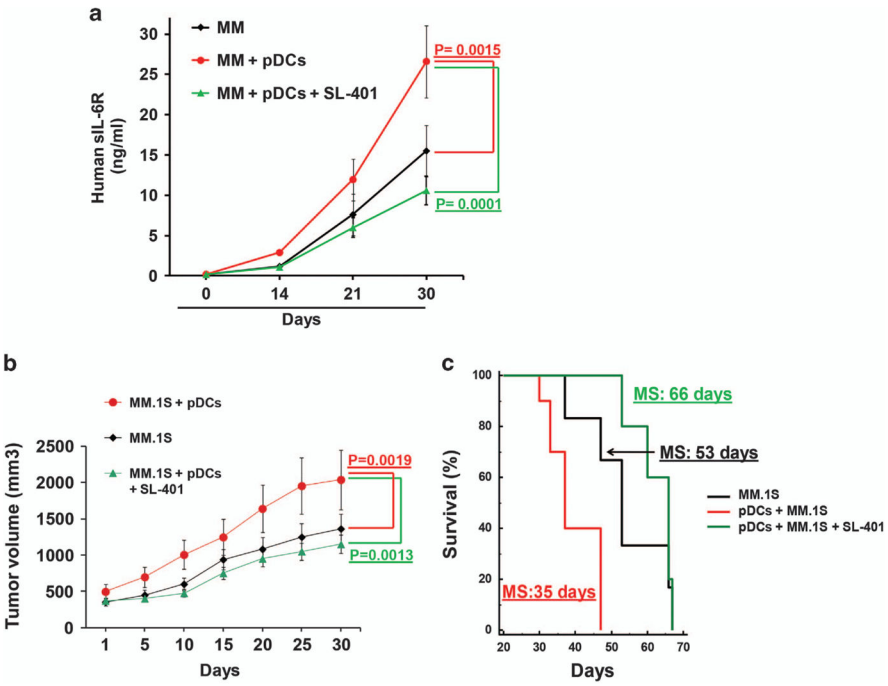

Figure 2.

SL-401 inhibits pDC-induced human MM cell growth *in vivo* and prolongs survival human MM xenograft model. (**a**) SCID-hu model: INA-6 MM cells (2×10^6 cells), alone or together with pDCs (0.4×10^6 cells) at 1:5 (pDC/MM) ratio, were injected directly into the human fetal bone implant in SCID-hu mice. Upon the first detection of human sIL-6R in mouse serum, mice were treated with vehicle control or SL-401 (12 μg/kg; IV) for 5 consecutive days for 1 week. Serum samples from 5 mice in each mice cohort were analyzed in duplicate using SpectraMax plate reader (mean ±s.d.; $P<0.05$; $n=2$) at the indicated times for quantification of human sIL-6 R (indicative of tumor burden) by ELISA. (**b** and **c**) Subcutaneous human MM xenograft model: CB-17 SCID-mice (**b**) were subcutaneously inoculated with MM.1 S cells (2.0×10^6), pDCs (0.4×10^6) or MM.1 S plus pDCs at 1:5 (pDC/MM) ratio in 100 μl of serum-free RPMI 1640 medium. When tumors were measurable (300 mm^3) at ~ 3 weeks after cell injection, mice (seven mice per group) were treated with vehicle alone or SL-401 (16 μg/kg, IV) for 5 consecutive days each week for 2 weeks. Tumor volume was measured two times per week. Mice were euthanized when tumor volume reached 2000 mm^3, and survival (**c**) is shown in a Kaplan–Meier plot. Median survival time for each group is shown (CI 95%; $P<0.0002$).

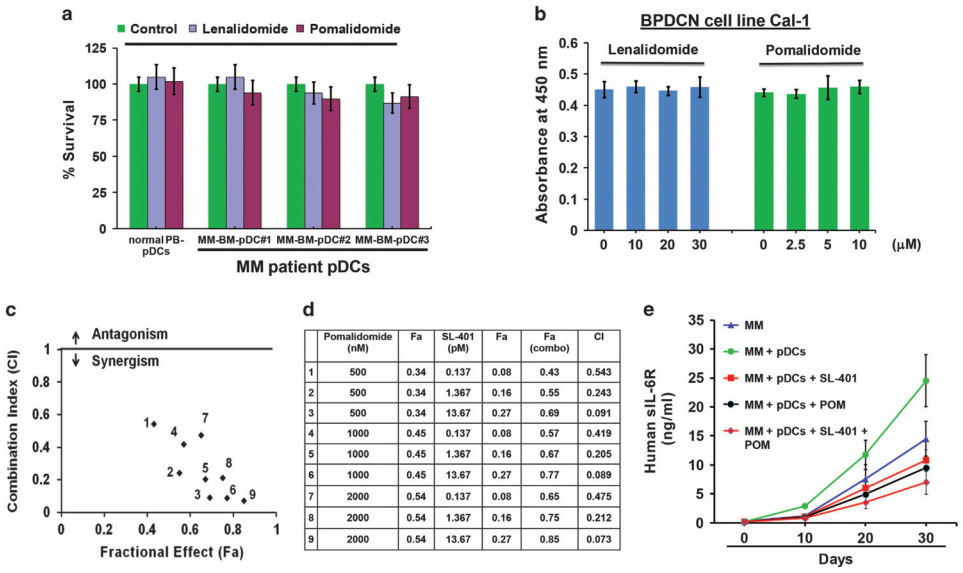

	Pomalidomide (nM)	Fa	SL-401 (pM)	Fa	Fa (combo)	CI
1	500	0.34	0.137	0.08	0.43	0.543
2	500	0.34	1.367	0.16	0.55	0.243
3	500	0.34	13.67	0.27	0.69	0.091
4	1000	0.45	0.137	0.08	0.57	0.419
5	1000	0.45	1.367	0.16	0.67	0.205
6	1000	0.45	13.67	0.27	0.77	0.089
7	2000	0.54	0.137	0.08	0.65	0.475
8	2000	0.54	1.367	0.16	0.75	0.212
9	2000	0.54	13.67	0.27	0.85	0.073

Figure 3.

Synergistic anti-MM activity of SL-401 and pomalidomide *in vitro* and *in vivo* (**a**) purified pDCs from MM patients BM (n =6) and normal donor PBMCs (n =3) were treated with DMSO (Control), Lenalidomide (30 μM), or Pomalidomide (10 μM) for 24 h, and analyzed for viability using trypan blue dye exclusion assay (mean ±s.d., P<0.05). (**b**) Blastic plasmacytoid dendritic cell neoplasm (BPDCN) cell line Cal-1 was treated with either DMSO (Control), or indicated concentrations of lenalidomide or pomalidomide for 48 h, and analyzed for viability using WST assays (mean ±s.d., P<0.05; n =3). (**c**) Co-cultures of MM.1 S cells and patient BM-pDCs at 1 pDC: 5 MM cell ratio were treated with indicated concentrations of SL-401, pomalidomide or SL-401 plus pomalidomide for 72 h and then analyzed for viability. Drug interactions at different combination concentrations were evaluated using Isobologram and Combination Index (CI) analyses. The graph (left) is derived from the values given in the Table (right). (**d**) Numbers 1–9 in graph represent combinations in Table. CI<1.0 indicates synergy. (**e**) INA-6 MM cells (2×10^6 cells), alone or together with pDCs (0.4×10^6 cells) at 1:5 (pDC/MM) ratio were injected directly into the human fetal bone implant in SCID-hu mice. Upon the first detection of human sIL-6R in mouse serum, mice (five mice per group) were treated with vehicle control, SL-401 (12 μg/kg; IV), pomalidomide (2.5 mg/kg; orally) or SL-401 plus pomalidomide for 2 weeks (SL-401: 5 consecutive days for first 1 week; pomalidomide: 4 consecutive days weekly for 2 weeks). Mouse sera samples were analyzed for human sIL-6R (indicative of tumor burden) using ELISA (mean ±s.d.; P<0.05; n =2).

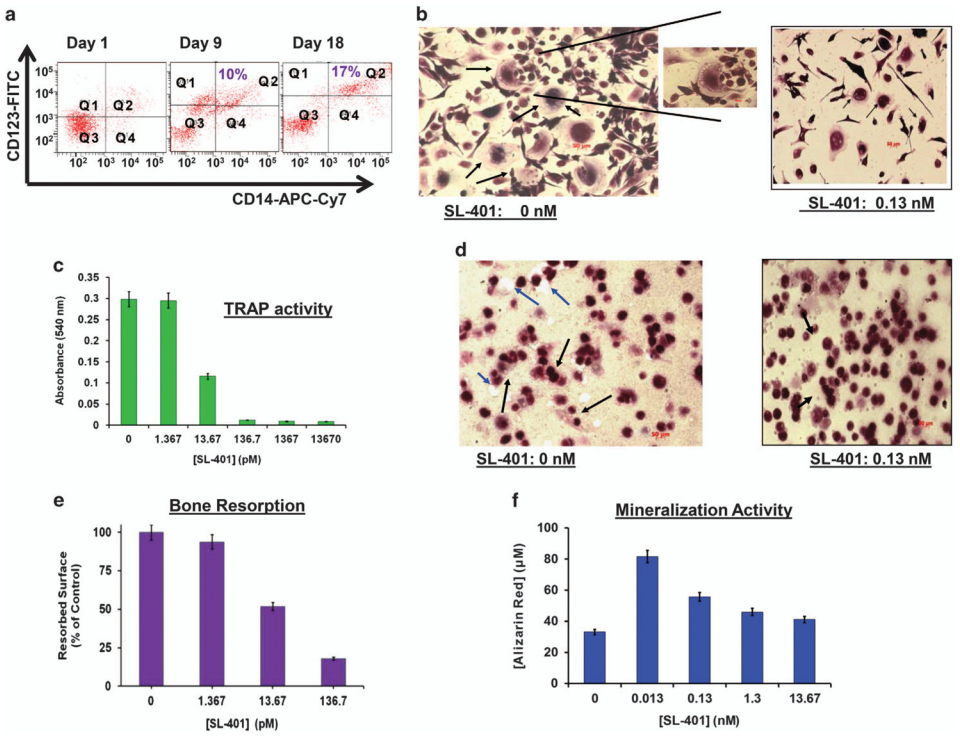

Figure 4.

Anti-osteolytic activity of SL-401. (**a**) $CD14^+$ monocytes isolated from MM patient PBMCs samples (n =5) were stimulated with hu-RANKL (40 ng/ml) and hu-M-CSF (25 ng/ml) for 3 weeks, with analysis of cells for CD123 (IL-3Rα) and CD14 at days 1, day 9 and day 18. (**b**) Monocytes derived from MM patient PBMCs were cultured with M-CSF and RANKL for 2 weeks to promote OCL differentiation, in the presence or absence of indicated concentrations of SL-401. OCLs were analyzed for tartrate-resistant acid phosphatase (TRAP) staining. Micrograph shows OCL formation in untreated vs SL-401-treated cells (black arrows indicate multi-nucleated OCL). (**c**) Monocytes derived from MM patient PBMCs were cultured with M-CSF and RANKL for 2 weeks to promote OCL differentiation, in the presence or absence of indicated concentrations of SL-401. TRAP activity was measured in supernatants of OCL culture by using a colorimetric substrate. A dose-dependent decrease in absorbance at 540 nm is indicative of the effect of SL-401 on OCL formation. SL-401 reduced number of $TRAP^+$ cells vs control culture (P<0.003). (**d**) OCL bone resorption was analyzed during OCL differentiation using OsteoAssay plates (dentine discs), in the presence or absence of SL-401. The captured images (**d**) of resorbed surface area were analyzed using NIH ImageJ software, and data (**e**) is presented as percentage of resorbed surfaces in untreated vs SL-401-treated cells. Black arrows in 'd' indicate multi-nucleated OCL, and blue arrows indicate resorbed pit on the OsteoAssay surface. (**f**) MM BM-derived OBLs were stimulated with ascorbic acid (0.05 mg/ml), β-glycerophosphate (2.16 mg/ml) and 10 nM of dexamethasone for 3 weeks in the presence or absence of indicated concentrations of SL-401, followed by assessment of bone mineralization (calcium deposits) using Alizarin Red staining (mean ±s.d.; n =4; P<0.05).

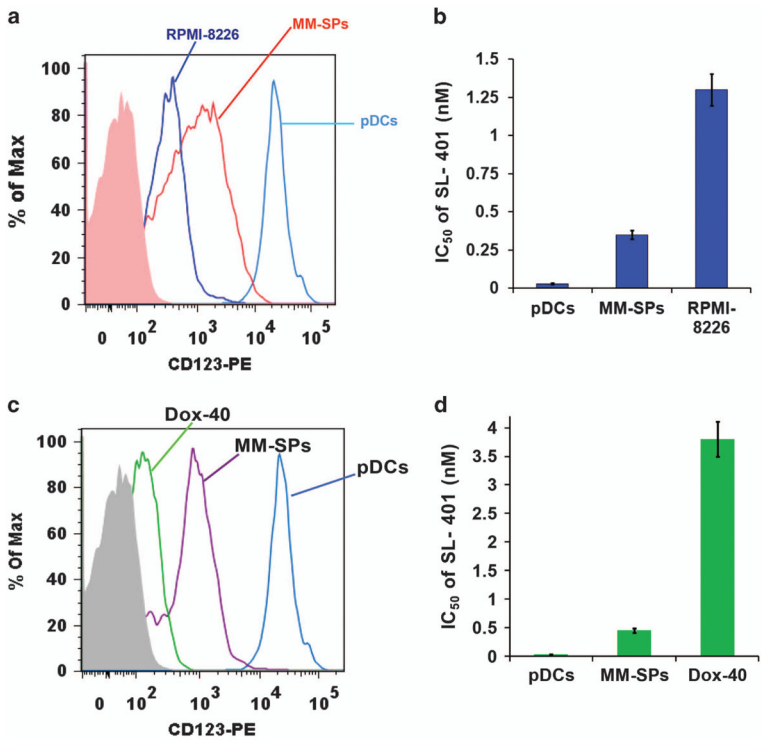

Figure 5.

Comparative analysis of SL-401 activity against clonogenic MM side population (MM-SPs) and MM cells (**a**) MM-SPs were isolated from RPMI-8226 using Hoechst 33342 staining (described in methods; ~ 99% purity). pDCs, MM-SPs and RPMI-8226 cells were analyzed for IL-3 R expression using anti-IL-3Rα-PE Abs and flow cytometry (mean ±s.d.; n =5). (**b**) RPMI-8226, MM-SPs and pDCs were treated with increasing concentrations of SL-401 for 48 h, and then analyzed for viability by WST assay. Bar graph shows IC_{50} of SL-401 against RPMI-8226, MM-SPs and pDCs (mean ±s.d.; n =5; P<0.005). (**c**) MM-SPs were isolated from RPMI-8226 R/Dox-40 using Hoechst 33342 staining (described in methods; ~ 99% purity). pDCs, MM-SPs and Dox-40 cells were analyzed for IL-3 R expression using anti-IL-3Rα-PE Abs and flow cytometry (mean ±s.d.; n =5). (**d**) Dox-40, MM-SPs, and pDCs were treated with increasing concentrations of SL-401 for 48 h and then analyzed for viability by WST assay. Bar graph shows IC_{50} of SL-401 against RPMI-8226 R/Dox-40, MM-SPs and pDCs (mean ± s.d.; n = 5; P <0.005).

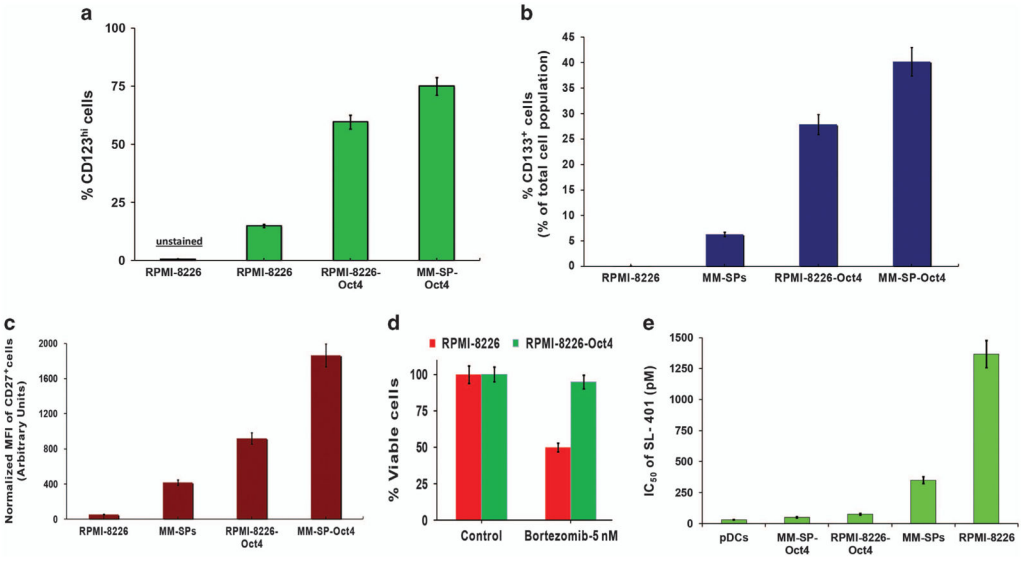

Figure 6.

Anti-cancer stem-like cell activity of SL-401 (**a**) RPMI-8226 cells were transfected with Oct4-GFP cDNA, and stably expressing Oct4^{+} RPMI-8226 cells (RPMI-8226-Oct4) were obtained by selecting transfected cells with G418 (0.5 mg/ml). After selection, cells were analyzed for GFP/CD123 double-positive populations in RPMI-8226-Oct4. RPMI-8226 and RPMI-8226-Oct4 cells were then analyzed for CD123/IL-3Rα^{hi} population by staining with anti-CD123/IL3Rα-PE Abs. Bar graph shows the frequency of IL-3Rα/CD123^{hi} populations (%CD123^{hi}) in RPMI-8226 and RPMI-8226-Oct4 cells. (**b** and **c**) MM-SPs stably expressing Oct4/GFP (MM-SP-Oct4) were derived as in 'A'. RPMI-8226, RMPI-8226-Oct4, MM-SPs, MM-SP-Oct-4 cells were analyzed for CD133^{hi} (**b**) or CD27^{hi} (**c**) populations by flow cytometry. Bar graph shows increased CD133^{+}- or CD27^{+}-expressing subpopulations in each cell type. (**d**) RPMI-8226 and RPMI-8226-Oct4 cells were treated with bortezomib for 48 h, and then analyzed for viability using WST assays (mean ±s.d.; n =3; P<0.005). (**e**) RPMI-8226, RMPI-8226-Oct4, MM-SPs and MM-SP-Oct-4 RPMI-8226 cells were treated with increasing concentrations of SL-401 for 48 h; cells were then stained with IL-3Rα/CD123 Ab, followed by quantification of viable CD123^{+} cells by flow cytometry. Bar graph shows IC_{50} of SL-401 against indicated cell type.